Kinetic and Mechanistic Study of the H-Transfer Reduction of Dimethyl Itaconate by a Rh/TPPTS Catalyst under Biphasic Conditions: Evidence for a Rhodametallacycle Intermediate

Nathalie Tanchoux[a] and Claude de Bellefon*[a]

Keywords: H-transfer / Kinetics / Reaction mechanisms / Biphasic catalysis / Rhodium / Metallacyclobutanes

The H-transfer reduction of dimethyl itaconate under biphasic catalysis using sodium formate/water as the hydrogen source with a Rh/TPPTS complex was studied. Labelling experiments reveal that the reduction proceeds through a 1,3-hydrogen addition. Kinetic studies allow us to propose a catalytic cycle going through a rhodametallacyclobutane intermediate with a rate-determining step involving sodium formate. A formal kinetic rate law was then derived from this mechanism which accounts for the results. This work evidences the switch between the mechanism of diacid reduction and that of the corresponding esters.

Introduction

The asymmetric hydrogenation of unsaturated substrates by either molecular hydrogen or H-transfer reduction is now one of the most important applications of homogeneous catalysis by chiral transition metal complexes.[1–4] Many studies report the use of optically pure phosphane complexes of Rh and Ru in organic[1,3] as well as in aqueous[2,5] or biphasic media.[6] The mechanisms of these reactions have been extensively studied, but very few details are known about the H-transfer reduction of α,β-unsaturated carboxylic esters using sodium formate/water in biphasic catalysis. As these reactions catalysed by chiral diphosphane complexes in aqueous medium are generally very complex, the racemic reduction of a prochiral substrate with a non-chiral monophosphane ligand was first studied. The kinetics of this reaction using dimethyl itaconate as a substrate and Rh/TPPTS as a catalytic complex were further investigated,[7] and labelling studies were undertaken in order to understand the mechanism and propose a catalytic cycle reflecting both the kinetic and mechanistic studies.

Results

Reaction

The reaction studied is the reduction of dimethyl itaconate (DMI) to dimethylmethylsuccinate (DMS) with sodium formate, catalysed by a water-soluble Rh complex in a biphasic medium (Equation 1). The catalytic system was generated by mixing the dimer $[Rh(cod)Cl]_2$ and the sodium salt of triphenylphosphanetrisulfonate (TPPTS) in an aqueous sodium formate solution.

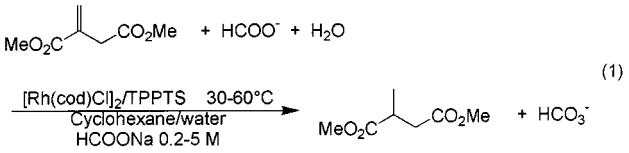

(1)

Analysis of the organic layer by gas chromatography and mass balance calculations confirm the near quantitative (> 95%) conversion of the substrate, DMI, into the product, DMS. A side product (< 5%) was detected and identified as an isomer of DMI, 2-dimethylmesaconate (DMM), formed by the shift of the double bond from the external to the internal position. Such an isomerisation of terminal to internal olefins has been frequently reported as a side reaction in for example hydrogenations.[8–10]

Liquid–Liquid Partition Equilibrium

As the course of the reaction is more conveniently followed by analysis of the organic phase, it is primordial to correlate the measured concentrations in the organic phase to the concentrations in the aqueous phase, since the latter is where the catalytic reaction actually takes place. The concentration of species A in the aqueous and organic layers were described by the linear relationship of Equation 2.

$$P_A = \frac{C^A_{Org}}{C^A_{Aq}} \qquad (m^3_{Aq} \cdot m^{-3}_{Org}) \tag{2}$$

All the measurements of partition coefficients have already been described in a previous paper.[7] The coefficients calculated from the experimental results are given in Table 1.

[a] Laboratoire de Génie des Procédés Catalytiques,
CNRS-CPE Lyon, URA 2211,
43, boulevard du 11 novembre 1918, B.P. 2077,
69616 Villeurbanne, France
Fax: (internat.) +33-4/72431673,
E-mail: Claude.de.Bellefon@lgpc.cpe.fr

  1434–1948/00/0707–1495 $ 17.50+.50/0

Table 1. Cyclohexane/water partition coefficients of DMI and DMS for various sodium formate concentrations at 293 K; a linear partition is observed for $0 \leq C_{Org}^{DMI} \leq 0.13$ kmol·m^{-3}

c_{HCOONa} [kmol·m$^{-3}_{Aq}$]	0	1	2.5	5
P_{DMI} [m$^3_{Aq}$·m$^{-3}_{Org}$]	1.2	2.8	4.3	11.3
P_{DMS} [m$^3_{Aq}$·m$^{-3}_{Org}$]	1.7	4	5.6	14

Kinetic Studies in a Well-Mixed Batch Reactor

The absence of mass transfer limitations in a well mixed batch reactor at 1100 rpm was previously checked.[11] A previous study[7] allowed the extraction of an activation energy of 71 kJ·mol^{-1}, in good agreement with those reported for other hydrogen transfer reductions of olefins.[12] The study also led us to propose the semi-empirical rate model of Equation 3, taking into account all the results obtained during that preliminary study.

$$r_{Aq} = \frac{kC_{Aq}^{Rh}C_{Aq}^{DMI}}{(KC_{Aq}^{DMI}+1)} \qquad (kmol.\,m_{Aq}^{-3}.s^{-1}) \qquad (3)$$

This model being based on preliminary results, it is only partial and does not take into account important parameters such as the concentrations of sodium formate or phosphane. More tests varying these parameters were performed in order to propose a more complete kinetic model that included the new information obtained. The range of conditions for this study is given in Table 2.

Table 2. Range of conditions for kinetic study in the batch reactor (other conditions: cyclohexane as organic phase solvent; stirring speed: 1100 rpm)

Concentration of catalyst [kmol·m$^{-3}_{Aq}$]	0.00132 to 0.005
Temperature [K]	303–313–323–333
Initial concentration of DMI in the organic phase [kmol·m$^{-3}_{Org}$]	0.024 to 0.144
Initial concentration of DMI in the aqueous phase [kmol·m$^{-3}_{Aq}$]	0.0021 to 0.013
Aqueous phase volume [10^{-6} m^3]	20 to 100
Organic phase volume [10^{-6} m^3]	10 to 20
Volume ratio α [m$^3_{Org}$·m$^{-3}_{Aq}$]	0.2 to 1
Concentration of sodium formate in the aqueous phase [kmol·m$^{-3}_{Aq}$]	0.2 to 5
TPPTS/Rh ratio	3.1 to 11.3

Formate decomposition in molecular hydrogen and sodium hydrogen carbonate has been noted, with or without substrate. This hydrogen production appears to be independent of the catalytic cycle of the DMI reduction. Tests have been performed under hydrogen pressures of 0.1 and 0.2 MPa to check for this, and no acceleration effect was noticed on the reduction rate. Thus, the DMI is not reduced by the molecular hydrogen formed from formate decomposition.

As seen in Figure 1, the observed initial reaction rate shows a first order dependence with respect to the catalyst concentration for formate concentrations of 5 and 1 kmol·m^{-3}.

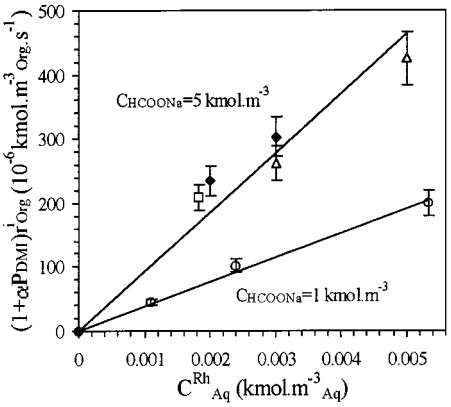

Figure 1. Influence of the catalyst concentration on the observed initial reaction rate r_{Org}^{i} [T = 313 K, C_{Org}^{DMI} = 0.155 kmol·m$^{-3}_{Org}$, TPPTS/Rh = 6; (◆ and ○): α = 1; (Δ): α = 0.5; (□): α = 0.45)

The influence of initial substrate concentration (Figure 2) on the observed initial rate shows an apparent zero order for the experiments carried out at a formate concentration of 1 kmol·m^{-3}, whereas it is complex for a concentration of 2.5 kmol·m^{-3} and close to an order of 1 for the most concentrated formate solution (5 kmol·m^{-3}).

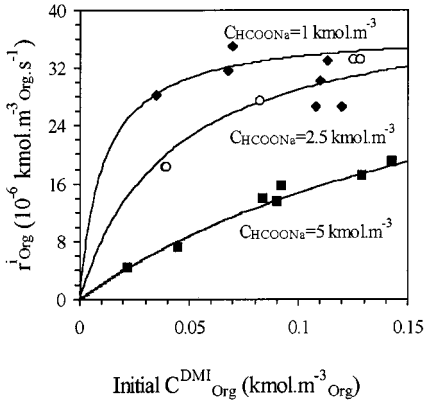

Figure 2. Influence of the initial substrate concentration on the observed initial reaction rate r_{Org}^{i} for different sodium formate concentrations (C_{Aq}^{Rh} = 0.002 kmol·m$^{-3}_{Aq}$, α = 1, TPPTS/Rh = 6, 313 K); the points represent the experimental data and the curves represent the semi-empirical model described by Equation 5

The effect of the phosphane on the initial rate exhibits a negative order with respect to the phosphane concentration, since the initial reaction rate decreases with increasing phosphane amounts in the aqueous phase (Figure 3).

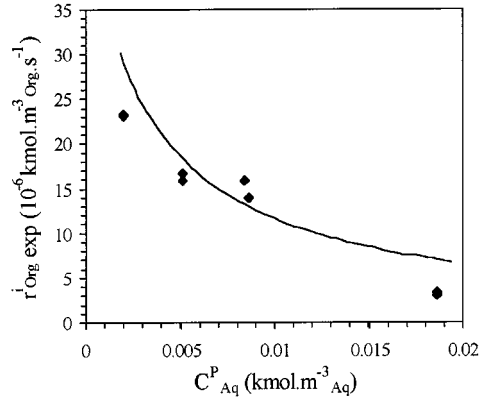

Figure 3. Influence of the phosphane concentration on the observed initial reaction rate r^{i}_{Org} (C^{DMI}_{Org} = 0.1 kmol·m$^{-3}_{Org}$, C^{Rh}_{Aq} = 0.002 kmol·m$^{-3}_{Aq}$, α = 1, C^{HCOONa}_{Aq} = 5 kmol·m$^{-3}_{Aq}$); the points represent the experimental data and the curves represent the semi-empirical model described by Equation 5

The influence of the sodium formate concentration was also studied, and it seems more complex. As shown in Figure 4, a linear increase of initial rate is observed until the formate concentration reaches 1 kmol·m$^{-3}_{Aq}$. Above this concentration, the rate decreases with increasing formate concentration. Such a complex behaviour has already been observed by Joó et al.[13] in the reduction of aldehydes by water-soluble phosphane complexes of ruthenium in biphasic medium. Joó evoked a salting-out effect due to the high formate concentration to explain this result. Formate concentration does indeed have a strong influence on the partition coefficients of the substrate and product (see Table 1).

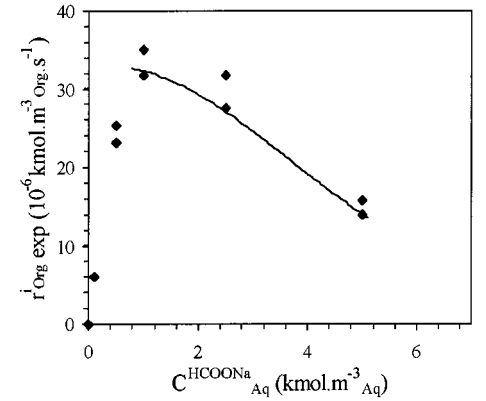

Figure 4. Influence of the sodium formate concentration on the observed initial reaction rate r^{i}_{Org} (C^{DMI}_{Org} = 0.1 kmol·m$^{-3}_{Org}$, C^{Rh}_{Aq} = 0.002 kmol·m$^{-3}_{Aq}$, α = 1, TPPTS/Rh = 6); the points represent the experimental data and the curves represent the semi-empirical model described by Equation 5

All these new results led us to propose a new semi-empirical model (Equation 4 and Equation 5), which represents all the experimental results rather well.

Knowing that $n_{DMI} = n^{DMI}_{Aq} + n^{DMI}_{Org}$, and from the mass balance in the batch reactor we can obtain

$$r_{Aq} = k\frac{C^{Rh}_{Aq}C^{DMI}_{Aq}}{\left(KC^{DMI}_{Aq} + C^{HCOO^-}_{Aq}C^{P}_{Aq}\right)} \quad (kmol.m^{-3}_{Aq}.s^{-1}) \quad (4)$$

$$-\frac{dC^{DMI}_{Org}}{dt} = r_{Org} = \frac{kC^{Rh}_{Aq}}{\left(1+\alpha P_{DMI}\right)}\frac{C^{DMI}_{Org}}{\left(\frac{K}{P_{DMI}}C^{DMI}_{Org} + C^{HCOO^-}_{Aq}C^{P}_{Aq}\right)} \quad (kmol.m^{-3}_{Org}.s^{-1}) \quad (5)$$

with α = volumetric ratio of the organic phase and the aqueous phase (m$^{3}_{Org}$·m$^{-3}_{Aq}$).

The kinetic parameters of the above model were estimated by means of a dynamic estimation and simulation software, able to perform numerical integrations using the entire concentration vs. time profiles and not only the initial rates of reaction.

As shown in Figure 2 to Figure 5 and Figure 6, the model fits rather well the experimental data except for low formate concentrations (< 1 kmol·m$^{-3}_{Aq}$). The results of the estimation are presented in Table 3.

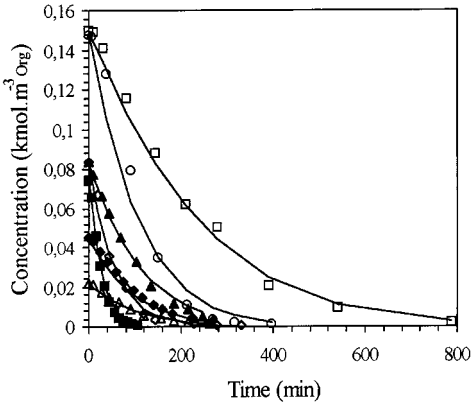

Figure 5. Concentration vs. time profiles. Comparison between experimental data (symbols) and semi-empirical model (lines). (Δ): Standard test: T = 313 K; C^{DMI}_{Org} = 0.1; C^{HCOONa}_{Aq} = 5, TPPTS/Rh = 6.3, α = 1, C^{Rh}_{Aq} = 0.002. Other tests: same with: (○) α = 0.2; (◆): α = 0.53, C^{Rh}_{Aq} = 0.005; (□): $C^{DMI}_{Org}(0)$ = 0.155, C^{HCOONa}_{Aq} = 1; (■): $C^{DMI}_{Org}(0)$ = 0.05, C^{HCOONa}_{Aq} = 2.5; (●): TPPTS/Rh = 3.1. Units: C^{DMI}_{Org} in kmol·m$^{-3}_{Org}$; C^{HCOONa}_{Aq} and C^{Rh}_{Aq} in kmol·m$^{-3}_{Aq}$; α in m$^{3}_{Org}$·m$^{-3}_{Aq}$.

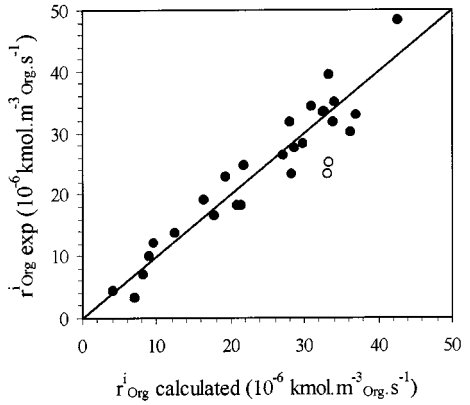

Figure 6. Calculated vs. experimental initial rates of reaction; conductions see Table 2 except for symbol (○) for which C^{HCOONa}_{Aq} = 0.5 kmol·m$^{-3}_{Aq}$

Table 3. Estimated kinetic constants and statistical analysis for the kinetic model determined from 30 experiments

	Value[a]	Confidence interval[b]
k [$m^3_{Aq}\cdot kmol^{-1}\cdot s^{-1}$]	0.053	0.048–0.058
K [$m^{-3}_{Aq}\cdot kmol^{-1}$]	2.1	1.8–2.4

[a] WRSS: weighted residual sum of squares for the parameter estimation: 1900. – [b] Interval at 95% confidence level.

Labelling Studies

This study was completed by labelling experiments, in order to determine the chemistry occurring, and maybe obtain a better understanding of the mechanism of this reaction. Table 4 gives the regioselectivity of the deuterium distribution in the products obtained by the reduction of DMI, carried out with $D_2O/HCOO^-$ first, then with $H_2O/DCOO^-$. Deuterium was never incorporated in the methyl ester groups.

Table 4. Amount of deuterium incorporated by the dimethyl methylsuccinate

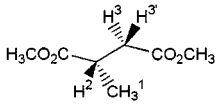

% labelled in position	H^1	H^2	H^3	$H^{3'}$
$D_2O/HCOO^-$	31±2	n.d.	58±3	47±2
$H_2O/DCOO^-$	13±3	n.d.	n.d.	n.d.

n.d.=not determined (<3%).

The extent of deuterium incorporation was determined by ^{1}H-NMR spectroscopy using the signal of the methoxy group as an internal standard (Figure 7).

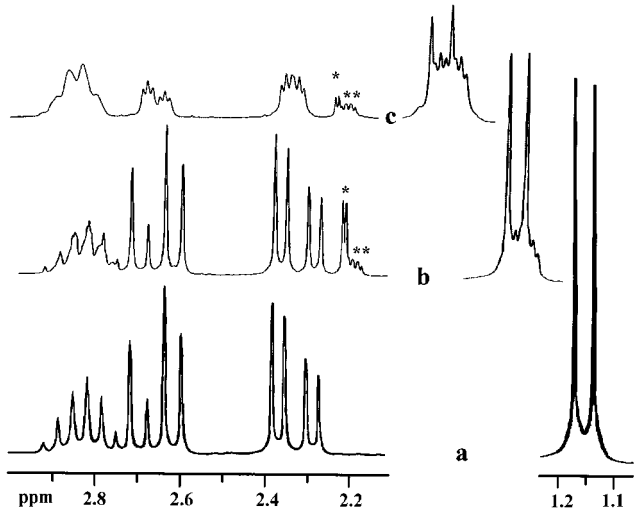

Figure 7. ^{1}H-NMR spectra of DMS (a) and of the products from reduction in $DCOONa/H_2O$ (b) and in $HCOONa/D_2O$ (c); signals of the vinylic proton in the by-product DMM: (*) **5**, (**) **6** (see Table 5)

In the case of reduction with $D_2O/HCOO^-$, the methine proton H^2 appears at δ = 2.84 as a broad multiplet (Figure 7c), showing no incorporation at this position. The two diastereotopic protons H^3 and $H^{3'}$ appear as two broad multiplets at δ = 2.33 and 2.65, corresponding to an AB system. Theses signals allowed us to determine a deuterium incorporation of 58 and 47% for each proton, respectively, i.e. a global quantitative deuterium incorporation at C^3. The methyl H^1 appears as a broad multiplet at δ = 1.14, showing a 31% deuterium incorporation at C^1. The $^{13}C\{^1H\}$-NMR spectra and DEPT sequence of the product confirmed there was no incorporation at the C^2 position. The triplet at δ = 37 corresponds to a quantitative monodeuteration –CHD in the C^3 position, confirmed by the DEPT sequence. The multiplet at δ = 16.7 shows an incorporation at the C^1 position. In the case of reduction with $H_2O/DCOO^-$, the ^{1}H-NMR spectra of DMS showed a broad multiplet at δ = 2.93 (Figure 7b) corresponding to the proton H^2, and showing no incorporation at this position. The two proton H^3 and $H^{3'}$ appeared as two doublets of doublets at δ = 2.4 and 2.72, corresponding to the coupling with the methine proton. These signals showed no deuterium incorporation at this position. The methyl appeared as a doublet and a small broad multiplet at δ = 1.21, showing 13% deuterium incorporation at C^1. The $^{13}C\{^1H\}$-NMR spectra and DEPT sequence confirmed these results. At δ = 35.7 and 37.4, two singlets showed no deuterium incorporation at C^2 and C^3, respectively. At δ = 16.7, C^1 appeared as a multiplet due to coupling with deuterium incorporated at this position.

Attempted Complex Characterization in situ

The ^{31}P-NMR spectrum of the catalytic complex in sodium formate shows broad signals centred at ca. δ = 31 and –5, probably due to a fluxional process including free TPPTS. Under catalytic conditions ([Rh] = 0.013 kmol·m^{-3}_{Aq}, TPPTS/Rh = 4), i.e. in the presence of sodium formate (3.3 kmol·m^{-3}) and DMI (0.02 kmol·m^{-3}), the NMR spectrum shows two types of compounds. The singlet at δ = 24.5 is assigned to a phosphonium according to previous reports.[14,15] It is formed by nucleophilic attack of the free TPPTS on the DMI, assisted by the Rhodium complex. Indeed, as proved in a separate experiment, the formation of the phosphonium is much slower when performed without Rhodium. Thus a yield of ca. 10%, based on TPPTS, is obtained without Rhodium, whereas a quantitative conversion of the free TPPTS is evidenced in the presence of the Rhodium complex. The change from fluxional to well defined ^{31}P spectra is thus attributed to the consumption of free TPPTS by DMI under catalytic conditions, which leads to the observation of the complex $[Rh(TPPTS)_3X]$ (X = Cl or OH)[16] based on the doublets and triplets at δ = 35.5 and 52.4 ($^1J_{Rh,P1}$ = 147 Hz, $^1J_{Rh,P2}$ = 182 Hz, and $^2J_{P1,P2}$ = 40 Hz), respectively. In water alone, under non-catalytic conditions, signals due to the complex $[Rh(TPPTS)_3(OH)]$, the phosphonium, and the TPPTS oxide are observed. A further signal at δ = 29.8 (d, $^1J_{Rh,P}$ = 145 Hz) is assigned to the cationic complex $[Rh(TPPTS)_2(cod)]^+$.[17]

Discussion

Mechanism

The results of labelling studies differ considerably from those obtained for mechanistic studies of slightly different systems, i.e. formic acid as the hydrogen source, itaconic acid as the substrate, or monophasic systems.[1–4]

The most surprising result was the absence of deuterium incorporation in the C^2 position while reducing the DMI in either a $D_2O/HCOO^-$ medium or in $H_2O/DCOO^-$. Very low incorporation of deuterium in the C^2 position has been reported recently in the H-transfer reduction of dimethyl itaconate with a Rh/diphosphane catalyst in DMSO.[18] This result indicates that the hydrogen atom incorporated in the C^2 position *must* come from the substrate dimethyl itaconate itself.

The mechanism of reduction is not likely to be close to the one proposed by Sinou[2] for the hydrogenation of DMI, as it was demonstrated that water did not play any role as a reactant, which is not the case here. Indeed, after reduction with $D_2O/HCOO^-$, the product DMS presented a 31% deuterium incorporation in the C^1 position and a complete monodeuteration in the C^3 position. As it is known that the exchange of hydrogen by deuterium in the formyl position is very slow compared to hydrogen transfer,[1] the incorporation of deuterium by the product cannot be attributed to $DCOO^-$, which is unlikely to be present in the catalytic phase.

When the reduction is carried out with $H_2O/DCOO^-$, a primary kinetic isotope effect of $k_H/k_D = 2.8$ is measured. This value, in agreement with those obtained by Brunner,[1] clearly shows that the sodium formate is involved in the rate-determining step.

The only mechanism accounting for all these experimental results seems to involve going through a rhodametallocyclobutane (Scheme 1). Only this type of intermediate allows the C^2 position to remain untouched, without any incorporation of deuterium, and only partial incorporation in the methyl group when reduction is carried out with $H_2O/DCOO^-$.

The first step of the mechanism is a de-coordination of one phosphane ligand to give a Rh complex containing two phosphane equivalents. Step **b** is the coordination of the olefin to the Rh complex. Step **c** is an intramolecular oxidative addition of the olefin to the rhodium complex, which gives a π-allyl rhodium hydride. This type of intermediate is very well-known in the π-allyl mechanism of olefin isomerization with complexes of palladium[19] and rhodium.[20] The formation of the phosphonium salt may well occur by nucleophilic attack of free TPPTS at the coordinated π-allyl, which supports the view of complex B being part of the cycle.

The next step is an intramolecular rearrangement of a π-allyl rhodium hydride complex to a rhodametallacyclobutane. The formation of such a complex with addition of hydride reagents to a π-allyl rhodium complex has already been reported.[21,22] Steps **b** to **d** consist of the shift of a hydrogen atom from position 3 to position 2. The resulting sp^2 carbon (C^2) is reduced to an sp^3 carbon *intramolecularly* before any possible exchange with the reaction medium. This mechanism is the only one we could propose that explains the results of the labelling experiments.

The formate then coordinates to the metallacyclobutane intermediate. Step **f** of hydride transfer from formate to rhodium has already been postulated for the mechanism of itaconic acid reduction by hydrogen transfer,[1] although it was not possible to decide whether it occurs externally or through an intramolecular pathway. It has been shown that in this type of rhodium hydride or dihydride intermediate, scrambling always occurs.[1,23] That explains very well the partial incorporation of deuterium (13%) at the C^1 position when the reduction is carried out with $H_2O/DCOO^-$. The

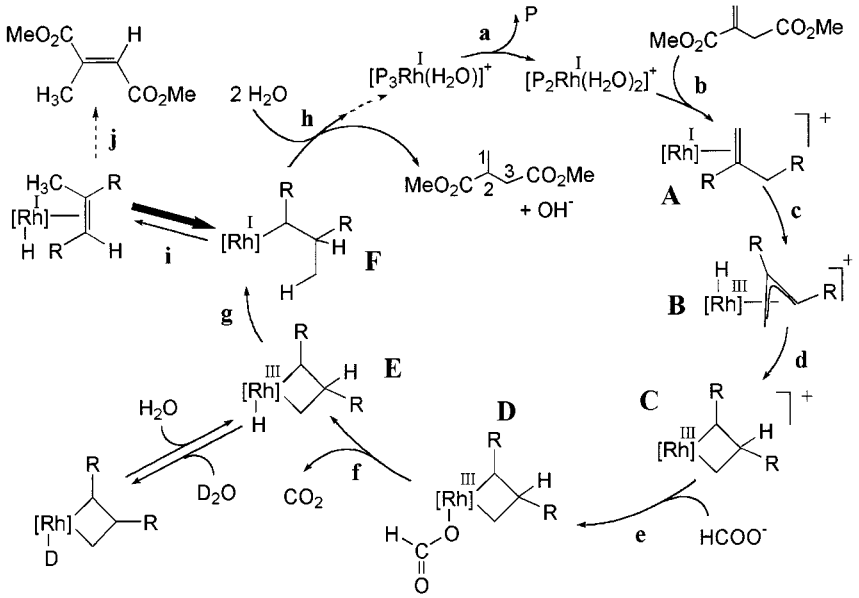

Scheme 1

exchange Rh-D/H_2O must be quite slow, as the incorporation obtained in the C^1 position (31%) is close to the theoretical incorporation (33%) with $D_2O/HCOO^-$.

Step **g** is an intramolecular reductive elimination that opens the metallacyclobutane and rapidly gives a rhodium alkyl intermediate. This type of equilibrium between a metallacycle and a metal alkyl intermediate has already been seen in such reactions as C–H activation,[24–26] the metal alkyl intermediate being thermodynamically more stable than the metallacycle hydride.[26]

The final product is then recovered by hydrolysis, which explains the quantitative incorporation observed at the C^3 position when the reduction is carried out with $D_2O/HCOO^-$. This result is confirmed by the lack of incorporation at C^3 when $H_2O/DCOO^-$ is used. Hydrolysis of alkyl complexes of transition metals such as palladium (II)[27] and selective incorporation of H^+ in Rh-alkyl fragments[28] has already been reported.

The by-product, dimethylmesaconate, is formed by an isomerisation of the substrate DMS by migration of the double bond from an external to an internal position. The *cis* isomer, dimethylcitraconate, is not formed (^{13}C and ^1H NMR). A similar secondary isomerisation reaction is reported for the reduction of itaconic acid with formic acid/triethylamine.[8] Curiously, in this case, the cis isomer, i.e. citraconic acid, is formed. In the by-product, only the methyl group (position 1) incorporates deuterium (10–15% with $H_2O/DCOO^-$ and 20–25% with $D_2O/HCOO^-$), which is in accordance with the position of step **i** in the proposed mechanism.

Kinetics

Choice of the rate determining step:

(i) The sodium formate is involved in or before the rate determining step as a primary kinetic isotope effect is noted when the reduction is carried out with $H_2O/DCOO^-$.

(ii) Hydrolysis occurs after the last rate determining step as no isotope effect is measured when the reduction is carried out with $D_2O/HCOO^-$.

(iii) Addition of sodium hydrogenocarbonate has no influence on the course of the reaction.[7] The CO_2, a product of the reaction, is not involved before the last rate determining step.

(iv) The liberation of one equivalent of phosphane ligand occurs before the last rate determining step, as addition of phosphane inhibits the reaction.

The last rate determining step is then step **f**, as it occurs after the formate coordination and before the liberation of CO_2 and the final, hydrolysis step. In addition, only the steps involving terminal products have been considered. Thus, steps **b** to **d** involving intermediates A, B, and C have been lumped in one step in the kinetics (Scheme 2), otherwise the kinetic rate law would have been more complex and would have induced more constants and larger uncertainty in their estimation. The X letter used represents intermediates A, B, and C (Scheme 2). The same process has been used for the steps **e** and **f**. The kinetic Scheme allowed us to derive a formal kinetic rate law for the formation of DMS using the Bodenstein approach for catalytic intermediates (Equation 6).

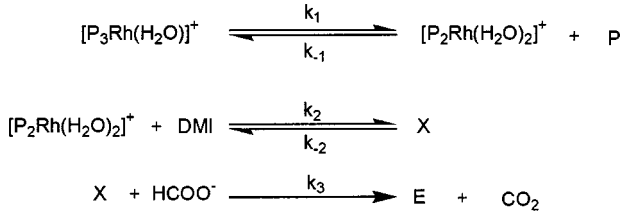

Scheme 2

$$r = k_3 \frac{C_{Aq}^{HCOO^-} C_{Aq}^{DMI} C_{Aq}^{Rh}}{\frac{k_{-2}}{k_2} + \frac{k_{-1}k_{-2}}{k_1k_2} C_{Aq}^{P} + C_{Aq}^{HCOO^-}\left(\frac{k_3}{k_2} + \frac{k_{-1}k_3}{k_1k_2} C_{Aq}^{P}\right) + C_{Aq}^{DMI}\left(1 + \frac{k_3}{k_1} C_{Aq}^{HCOO^-}\right)} \quad (6)$$

This rate law is in accordance with experimental results, i.e. a negative order with respect to phosphane, first order with respect to the catalyst concentration, and complex order with respect to the substrate. It was not possible, however, to take into account the influence of the sodium formate concentration. The semi-empirical model (Equation 4 and Equation 5) presents a negative order with respect to the formate concentration, whereas the formal kinetic rate law presents a positive order of between 0 and 1.

Although this expression gives a complex order with respect to formate concentration, it was not possible to take its influence into account over the whole range of concentration used for the kinetic study.

The model is in good agreement with the experiments, but it was not possible to estimate one set of kinetic parameters for both series of experiments with sodium formate concentrations of 5 and 1 $kmol \cdot m^{-3}$. In addition, as the model possesses an intrinsic inaccuracy due to constants coupling, it was not possible to determine values of intrinsic kinetic constants with a sufficient accuracy, but only ratios of constants. More tests under a wider range of conditions where kinetic constants would not be coupled need to be performed.

Conclusion and Future Work

The kinetic and mechanistic study of H-transfer reduction of dimethyl itaconate by sodium formate/water under biphasic catalysis has been presented. A complex, semi-empirical kinetic model was first validated. It exhibits complex order with respect to the substrate concentration, and inhibition by the phosphane. Numerical integration using the entire concentration vs. time profiles provided values for the kinetic parameters of this model. Labelling studies and ^1H- and ^{13}C-NMR analysis were also performed. A catalytic cycle has been proposed based on these results. A rhodametallacyclobutane intermediate best accounts for the systematic non-deuteriation of the C^2 position of the product, the reduction being carried out either by $H_2O/DCOO^-$ or $D_2O/HCOO^-$. The mechanism is also supported by the good fit between the empirical model and the formal rate law, de-

rived from the mechanistic steps, despite a poor agreement concerning the influence of sodium formate.

The main conclusion concerns the shift in the mechanism on going from diacids to their ester derivatives. Unsaturated acids reduction proceeds through a *cis*-1,2-hydrogen addition,[1,8] whereas this work shows that reduction of esters should undergo a 1,3-addition.[1] This switch in mechanism may well account for the lower optical yields observed in the enantioselective H-transfer reduction of esters compared to their corresponding acids.[8]

Experimental Section

General: ^{31}P-NMR spectra (external reference H_3PO_4 85% D_2O) were recorded on a Bruker AM 300 (121.51 MHz) and a Bruker AM 200 (81.015 MHz). ^{1}H- and ^{13}C-NMR spectra (external reference $SiMe_4$) were recorded on a Bruker AM 200 (200.13 MHz and 50.32 MHz, for ^{1}H and ^{13}C, respectively). Deuterated water (99.9 atom% D, Aldrich) and [D_2]formic acid (99+ atom%, 95% in D_2O, ACROS) for the labelling study were degassed and used without further purification. – TPPTS 30% wt in water, sodium formate (97%, Aldrich), dimethyl itaconate (97%, Aldrich), decane (99%, Aldrich), mesaconic acid (99%, Aldrich), and the catalyst precursor [Rh(cod)Cl]$_2$ (98%, Strem) were used as received. All the experiments were performed under argon or nitrogen. – Partition isotherms determination: The experimental procedure for determining partition isotherms has already been described in a previous paper.[7] – Kinetic studies in a well mixed batch reactor: All the details have already been described in a previous paper.[7] The reduction of dimethyl itaconate (DMI) was performed under a range of conditions, given in Table 2. The initial rate of reaction is calculated from the slope of concentration vs. time profiles at low conversion (< 10%).

Labelling Study/Reduction of DMI in D_2O/HCOONa: A solution of TPPTS in water (30% wt, 2 cm^3, 1.22 mmol) was evaporated. D_2O (2 cm^3) was then added to the residue, and the procedure was repeated twice. A solution of sodium formate in D_2O (5, 8 cm^3, 40 mmol) was then added to an orange slurry of [Rh(cod)Cl]$_2$ (48.9 mg, 0.2 mmol) in the solution of TPPTS in D_2O previously prepared. The mixture was stirred at room temperature for about 12 h and stored at 4 °C. The catalytic run was performed as previously described.[7] After reduction, the organic layer was separated, dried with $CaCO_3$, and the solvent was evaporated. The oily product was analysed by NMR spectroscopy. – ^{13}C NMR: δ = 16.7 (m, $^1J_{CD}$ = 19.7 Hz, C^1), 35.5 (m, C^2), 37.0 (t, $^1J_{CD}$ = 20.0 Hz, C^3), 51.5 (s, C^7), 51.8 (s, C^5), 172.1 (s, C^6), 175.5 (s, C^4). – ^{1}H NMR data for the isotopomers identified in the organic layer: **1**: δ = 1.15 (d, $^3J_{12}$ = 7.1 Hz, 3 H, H^1), 2.65 (dt, $^3J_{32}$ = 8.0 Hz, $^2J_{HD}$ = 2.3 Hz, 1 H, H^3), 2.80 (m, 1 H, H^2), 3.61, 3.63 (s, 3 H, H^5, H^7). – **2**: δ = 1.15 (d, $^3J_{12}$ = 7.1 Hz, 3 H, H^1), 2.33 (m, $^3J_{3'2}$ = 6.0 Hz, $^2J_{HD}$ = 2.3 Hz, 1 H, H$^{3'}$), 2.80 (m, 1 H, H^2), 3.61, 3.63 (s, 3 H, H^5, H^7). – **3**: δ = 1.13 (dt, $^3J_{12}$ = 7.1 Hz, $^2J_{HD}$ = 1.8 Hz, 2 H, H^1), 2.65 (dt, $^3J_{32}$ = 8.0 Hz, $^2J_{HD}$ = 2.3 Hz, 1 H, H^3), 2.80 (m, 1 H, H^2), 3.61, 3.63 (s, 3 H, H^5, H^7). – **4**: δ = 1.13 (dt, $^3J_{12}$ = 7.1 Hz, $^2J_{HD}$ = 1.8 Hz, 2 H, H^1), 2.33 (m, $^3J_{3'2}$ = 6.0 Hz, $^2J_{HD}$ = 2.3 Hz, 1 H, H$^{3'}$), 2.80 (m, 1 H, H^2), 3.61, 3.63 (s, 3 H, H^5, H^7). – **5**: δ = 2.22 (d, $^4J_{13}$ = 1.5 Hz, 3 H, H^1), 3.74, 3.70 (s, 3 H, H^5, H^7), 6.71 (broad, 1 H, H^3). – **6**: δ = 2.22 (m, $^4J_{13}$ = 1.5 Hz, $^2J_{HD}$ = 1.46 Hz, 2 H, H^1), 3.74, 3.70 (s, 3 H, H^5, H^7), 6.71 (broad, 1 H, H^3).

Labelling Study/Reduction of DMI in H_2O/DCOONa: A solution of [D_2]formic acid in D_2O (95% wt, 10 g, 0.19 mmol) was added to an aqueous solution of sodium hydroxide (10, 20 cm^3, 0.2 mmol). The mixture was then evaporated and water was added to the residue. This procedure was repeated twice to remove traces of D_2O and D^+. Water (40 cm^3) was finally added to the thus prepared [D]sodium formate. Preparation of the catalyst and realization of the kinetic tests were then performed as already described.[7] – After reduction the organic layer was separated, dried with $CaCO_3$, and the solvent was evaporated. The oily product was analyzed by NMR spectroscopy. – ^{13}C NMR: δ = 16.7 (m, $^1J_{CD}$ = 19.7 Hz, C^1), 35.7 (m, C^2), 37.4 (s, $^1J_{CD}$ = 20.0 Hz, C^3), 51.7 (s, C^7), 51.9 (s, C^5), 172.3 (s, C^6), 175.7 (s, C^4).

The ^{1}H-NMR data showed the presence of isotopomers **5**, **6**, **7**, and **8**. – **7**: δ = 1.16 (d, $^3J_{12}$ = 7.1 Hz, 3 H, H^1), 2.35 (dd, $^2J_{33'}$ = 16.3 Hz, $^3J_{23'}$ = 6.0 Hz, 1 H, H$^{3'}$), 2.67 (dd, $^3J_{23}$ = 8.0 Hz,1 H, H^3), 2.85 (m, 1 H, H^2), 3.61, 3.63 (s, 3 H, H^5, H^7). – **8**: δ = 1.16 (dt, $^3J_{12}$ = 7.1 Hz, $^2J_{HD}$ = 1.9 Hz, 2 H, H^1), 2.35 (dd, $^2J_{33'}$ = 16.3 Hz, $^3J_{23'}$ = 6.0 Hz, 1 H, H$^{3'}$), 2.67 (dd, $^3J_{23}$ = 8.0 Hz, 1 H, H^3), 2.85 (m, 1 H, H^2), 3.61, 3.63 (s, 3 H, H^5, H^7).

Synthesis of the By-Product DMM: A drop of sulfuric acid 98% was added to a solution of mesaconic acid (2 g, 15.3 mmol) in methanol (50 cm^3). The mixture was stirred at room temperature for 3 days. The solvent was then evaporated and the crude product obtained was characterised by ^{1}H-NMR (200 MHz, $CDCl_3$) spectroscopy. – ^{1}H NMR: δ = 2.30 (d, $^4J_{13}$ = 1.6 Hz, 3 H, H^1), 3.78, 3.82 (s, 3 H, H^5, H^7), 6.80 (q, 1 H, H^3).

Acknowledgments

The authors are grateful to the Région Rhône-Alpes, the Centre National de la Recherche Scientifique and the Rhône-Poulenc com-

Table 5. Different isotopomers/isomers present in organic layers after labelling experiments

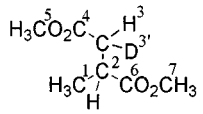 **1**	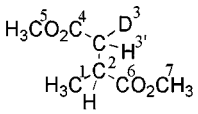 **2**	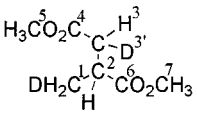 **3**	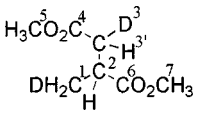 **4**
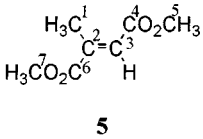 **5**	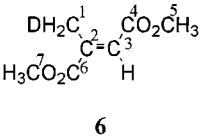 **6**	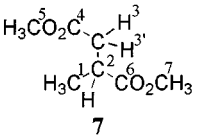 **7**	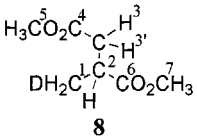 **8**

pany for financial support. N. T. is also grateful to the Région Rhône-Alpes for a PhD grant.

[1] W. Leitner, J. Brown, H. Brunner, *J. Am. Chem. Soc.* **1993**, *115*, 152–159 and references therein.
[2] A. Bucsai, J. Bakos, M. Laghmari, D. Sinou, *J. Mol. Catal. A: Chemical* **1997**, *116*, 335–342.
[3] D. Heller, R. Kadyrov, M. Michalik, T. Freier, U. Schmidt, H. W. Krause, *Tetrahedron: Asymmetry* **1996**, *7*, 3025–3035.
[4] A. Harthun, R. Kadyrov, R. Selke, J. Bargon, *Angew. Chem. Int. Ed. Engl.* **1997**, *36*, 1103–1105.
[5] K. T. Wan, E. Davies, *Tetrahedron: Asymmetry* **1993**, *4*, 2461–2468.
[6] Y. Amrani, L. Lecomte, D. Sinou, *Organometallics* **1989**, *8*, 542–547.
[7] C. de Bellefon, N. Tanchoux, S. Caravieilhes, D. H. Schweich, *Catal. Today* **1999**, *48*, 211–219.
[8] H. Brunner, W. Leitner, *J. Organomet. Chem.* **1990**, *387*, 209–217.
[9] X. Wang, L. K. Woo, *J. Mol. Catal. A: Chemical* **1998**, *130*, 171–176.
[10] T. Karlen, A. Ludi, *Helv. Chim. Acta* **1992**, *75*, 1604–1606.
[11] C. de Bellefon, N. Tanchoux, S. Caravieilhes, *J. Organomet. Chem.* **1998**, *567*, 143–150.
[12] R. A. W. Johnstone, A. H. Wilby, *Chem. Rev.* **1985**, *85*, 129–170.
[13] A. Bényei, F. Joó, *J. Mol. Catal.* **1990**, *58*, 151–163.
[14] C. de Bellefon, E. Pollet, P. Grenouillet, *J. Mol. Catal. A: Chemical* **1999**, 145, 121–126.
[15] M. Hernandez, P. Kalck, *J. Mol. Catal. A: Chemical* **1997**, *116*, 131–146.
[16] W. A. Herrmann, J. A. Kulpe, W. Konkol, H. Bahrmann, *J. Organomet. Chem.* **1990**, *389*, 85–101.
[17] R. R. Schrock, J. A. Osborn, *J. Am. Chem. Soc.* **1971**, *93*, 2397–2407.
[18] S. Lange, W. Leitner, R. Mynott, C. Wirtz, XIth International Symposium on Homogeneous Catalysis, St. Andrews, Scotland, July **1998**, p. 73.
[19] G. W. Parshall, S. D. Ittel, *Homogeneous Catalysis: The Applications and Chemistry of Catalysis by Soluble Transition Metal Complexes*, 2nd ed., Wiley-Interscience publication, **1993**, p. 14–16.
[20] K. E. Koenig, W. S. Knowles, *J. Am. Chem. Soc.* **1978**, *100*, 7561–7564.
[21] R. A. Periana, R. G. Bergman, *J. Am. Chem. Soc.* **1984**, *106*, 7273–7274.
[22] R. A. Periana, R. G. Bergman, *J. Am. Chem. Soc.* **1986**, *108*, 7346–7355.
[23] D. J. Hardick, I. S. Blagbrough, B. V. L. Potter, *J. Am. Chem. Soc.* **1996**, *118*, 5897–5903.
[24] T. H. Tulip, D. L. Thorn, *J. Am. Chem. Soc.* **1981**, *103*, 2448–2450.
[25] W. D. Jones, F. J. Feher, *J. Am. Chem. Soc.* **1984**, *106*, 1650–1663.
[26] R. H. Crabtree, *Chem. Rev.* **1985**, *85*, 245–269.
[27] S. Ganguly, D. Roundhill, *Organometallics* **1993**, *12*, 4825–4832.
[28] C. Detellier, G. Gelbard, H. B. Kagan, *J. Am. Chem. Soc.* **1978**, *100*, 7556–7561.

Received August 27, 1999
[I99314]